Nuclear Science and Techniques **22** (2011) 272–276

Electronic structure of In_2O_3 nanowires synthesized at low temperature

YUAN Gang[1,2] GAO Jing[2] SUN Xuhui[2,*] ZHOU Xingtai[1]

[1]*Shanghai Institute of Applied Physics*, *Chinese Academy of Sciences*, *Shanghai 201800, China*

[2]*Institute of Functional Nano and Soft Materials*, *and Jiangsu Key Laboratory for Carbon-based Functional Materials and Devices*, *Soochow University*, *Suzhou 215123*, *China*

Abstract In_2O_3 nanowires with uniform morphology and single crystalline structure were synthesized at low temperature of 400ºC~450ºC using InSb as the precursor *via* VLS mechanism. The nanowires have uniform diameter of about 40 nm and are up to tens of micrometres in length and grew along the [100] direction as established by high resolution electron microscopy. The electronic and local structures of In_2O_3 nanowires, compared to that of In_2O_3 powder, have been studied with X-ray absorption fine structure (XAFS) at In K-edge and O K-edge. The XAFS results reveal the stronger In-O bonding in In_2O_3 nanowires compared to bulk In_2O_3.

Key words In_2O_3 nanowires, Low temperature synthesis, XAFS, Electronic structure

1 Introduction

One-dimensional metal oxides semiconductor nanostructures have attracted great interests due to their distinctive electronic and optical properties[1,2]. Among them, indium oxide (In_2O_3) nanowire with a direct wide band-gap (3.55–3.75 eV) is an important transparent conducting oxide material and has been used in electronics, optoelectronics, photo-detectors, memory devices, and high sensitivity sensors, because of their unique optical[3], chemical[4] and electronic[5] properties. In_2O_3 nanowires have been synthesized in various ways and used in gas sensors for detecting gases of acetone, ammonia, NO_2, ethanol, hydrogen, ozone, etc[6-11]. The nanowires exhibit good transistor characteristics with well-defined linear and saturation regions with on/off ratios as high as 3×10^4 at 0.1-V drain bias, electron carrier density of 3.7×10^{17} cm^{-3} and electron mobility of 85 cm^2/Vs[12]. Some In_2O_3 nanowires emit stable and high brightness blue light under excitation at 260 nm[13], and others have a strong PL emission in UV region under UV lights[14]. All these properties should be related to electronic and local structures of In_2O_3 nanowires, which are of great importance for design and fabrication of In_2O_3 nanowire-based nanodevices, hence the need of further investigations.

In_2O_3 nanowires have been grown under mainly the vapor-solid (VS)[15] and vapor-liquid-solid (VLS)[16] mechanisms. In most of the In_2O_3 nanowire synthesis, metal indium or In_2O_3 powder is used as the precursor. However, the synthesis with In_2O_3 powder must be performed at about 1000°C[17], because the In_2O_3 powder, which melts at 1910°C, sublimates at temperatures above 850°C. Metal indium is of low melting point, but it becomes In_2O_3 easily during the synthesis process, and high temperature is still needed to synthesize In_2O_3 nanowires[3].

Some methods have been employed to reduce the synthesis temperature, such as using Ag catalyst to lower the growth temperature to 700°C[18], or using water to oxidize indium and synthesize In_2O_3 nanobelts at 600°C–850°C[19]. For nanoelectronics applications, however, it is still a challenge to synthesize In_2O_3 nanowires at complementary metal-oxide-semiconductor (CMOS) compatible temperature (<450°C). The In_2O_3 nanowires synthesis

---

Supported by National Basic Research Program of China (973 program 2010CB934500) and National Nature Science Foundation of China (Grant No.: 51072127)

* Corresponding author. *E-mail address:* xhsun@suda.edu.cn

Received date: 2011-03-09

at moderate conditions, which requests less equipment and power consumption, will facilitate its integration into the semiconductor industry.

To achieve low temperature synthesis of In_2O_3 nanowires, we used InSb, as the starting material, instead of In_2O_3 powder or metal indium as precursors. The In_2O_3 nanowires were synthesized below 450°C, with uniform morphology and single crystalline structure. Electronic and local structures of the In_2O_3 nanowires were investigated on synchrotron radiation facilities, with synchrotron radiation X-ray diffraction (XRD), and X-ray absorption fine structure (XAFS), i.e. X-ray absorption near-edge structure (XANES) and extended X-ray absorption fine structure (EXAFS). The synchrotron radiation techniques are powerful tools for studying electronic and optical properties of one-dimensional semiconductor nanomaterials[20,21].

2 Experimental

In_2O_3 nanowires growth was carried out in a horizontal tube furnace system, with a quartz tube, and an alumina crucible. InSb powder (99.99%, Alfa Aesar) was placed in middle of the high-temperature zone of the furnace. Si wafer deposited with 10-Å gold film or 30-nm gold nanoparticles as catalyst was positioned downstream as the target substrate for nanowire growth. The tube was evacuated to 5 Pa prior to the experiment. Argon as the carrier gas was introduced at one end of tube at 100 sccm (standard cubic centimeters per minute) and the system was kept at 2×10^4 Pa during the entire growth process, so as to reduce indium oxidation by the residual air. The furnace temperature was increased at the rate of 40°C min^{-1} to 500°C–600°C and kept there for 60 min. Temperature of the nanowires growth zone was 400°C–450°C as monitored by a thermocouple.

Morphology and structure of the as-synthesized nanowires were characterized by scanning electron microscopy (SEM) (FEI Quanta FRG 200F) equipped with energy dispersive X-ray spectroscopy (EDS) and high-resolution transmission electron microscopy (HRTEM) (FEI Tecnai G2 F20 S-TIWN). Crystal structures of the as-synthesized products were obtained by XRD at BL14B1 beamline of Shanghai Synchrotron Radiation Facility (SSRF). The In K-edge and O K-edge XAFS of the In_2O_3 nanowires were obtained at the BL14W1 beamline (4–29 keV) at SSRF and the SGM beamline (250–1900 eV) at Canadian Light Source (CLS), respectively.

3 Results and discussion

Figure 1a shows an SEM image of the as-synthesized In_2O_3 nanowires on a Si substrate, revealing high-yield nanowire growth. The nanowires are of uniform size, about 40 nm in diameter and up to tens of micrometres in length. Composition of the In_2O_3 nanowires was confirmed by EDS spectra (not shown here), where only indium and oxygen were detected. The XRD patterns in Fig.1b clearly show that the In_2O_3 nanowires have a body-centered cubic (bcc) structure with a lattice constant of a=10.50 Å, in good agreement with the value reported for bcc In_2O_3 (JCPDS 6-0416, a=10.11 Å). Structures of the In_2O_3 nanowires were further characterized with HRTEM. Fig.1c shows a typical HRTEM image of an In_2O_3 nanowire with a diameter of about 35 nm along its entire length. The inset is the selected area electron diffraction (SAED) of the nanowire, revealing that it is a single crystal with bcc structure. The HRTEM image shows that the In_2O_3 nanowire is a high quality single crystal and contains no noticeable defects such as dislocations and stacking faults. The interplane spacings of 0.72 nm and 0.51 nm correspond to d-spacing of $(0\bar{1}1)$ and (200) crystal planes of bcc structure, respectively, and the growth direction of the nanowire is along [100].

The growth of In_2O_3 nanowires follows the vapor-liquid-solid (VLS) mechanism, evidenced by the observation of metal nanoparticles at the tips of the nanowires. Fig.2a shows a typical TEM image of an individual In_2O_3 nanowire with a round dark particle. Local point EDS analysis (Fig.2b), with a focused TEM beam spot of 9 nm on the targeted sample area, shows that the particle, the dark ball on the nanowire tip, is composed primarily of Au, In, Sb and O, and the nanowire part (Fig.2c) is composed of only In and O in an approximately 2:3 atomic ratio. No Sb was detected in the nanowire part at EDS detection limit. The XAFS analysis found no Sb residual, either, in the In_2O_3 nanowires. The C and Cu signals in the spectra are from the carbon-coated copper grid of the TEM.

The Sb existing in the tip particle suggests that evaporated InSb might transport to the substrate without oxidation, and form Au-InSb liquid alloy at 400–450°C via the following reaction, at the eutectic temperature of 420°C for Au-In-Sb alloy[22,23],

$$Au(s)+InSb(g)\rightarrow Au_xIn\text{-}InSb\text{-}Sb(l) \qquad (1)$$

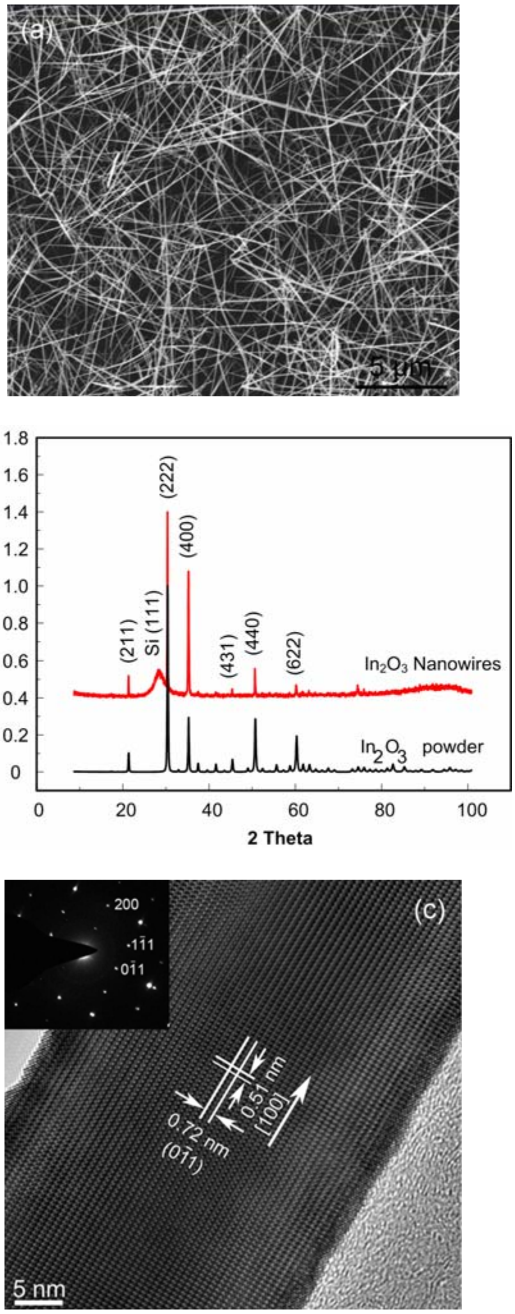

Fig.1 (a) Typical scanning electron microscopy (SEM) image of as-synthesized In_2O_3 nanowires grown on a Si substrate. (b) XRD pattern of In_2O_3 nanowires. (λ =1.2438 Å convert to λ =1.54 Å). (c) HR-TEM image of the In_2O_3 nanowire.

The oxidation of indium to In_2O_3 and the volatility of Sb then occurred in the liquid alloy. Sb is easy to volatile under the growth condition, and all Sb were brought out of the system. When In_2O_3 concentration in the liquid alloy was supersaturated, solid In_2O_3 were crystallized from the liquid alloy to form the nanowire. The low melting point of InSb and low eutectic point of Au-InSb alloy make it possible to grow In_2O_3 nanowires at temperatures below 450°C.

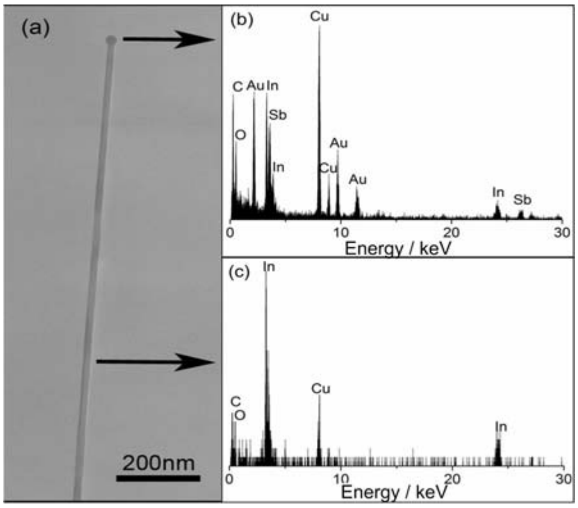

Fig.2 (a) TEM image of the In_2O_3 nanowire with a metal tip. (b) EDX analysis on the tip of the nanowire. (c) EDX analysis on the body of the nanowire.

Electronic and local structures of the In_2O_3 nanowires were studied with XAFS, by measuring and interpretating absorption coefficient above a specific absorption edge, in this case, the K-edges of indium and oxygen. Fig.3a shows the In K-edge XAFS of as-prepared In_2O_3 nanowires, compared with that of In_2O_3 crystalline powder sized at several micrometers with bcc structure, which is regarded as bulk In_2O_3. The XAFS, of In_2O_3 nanowires resembles that of bulk In_2O_3 powder, demonstrating that they have essentially the same bcc lattice. The inset is the normalized K-edge XANES, where the absorption edge jump of In_2O_3 nanowires is slightly higher than that of In_2O_3 powder. This reveals that the In_2O_3 nanowirs have more outermost empty electron orbits (5*p*) of indium than that of bulk In_2O_3. More electrons at 5*p* orbits of indium approach to the orbits of O, that is, stronger bonding between In and O is formed in In_2O_3 nanowirs than in bulk In_2O_3.

Figure 3b shows the Fourier transform of the EXAFS with k weighting (data range: k = 2.5–14 Å^{-1} for In_2O_3 nanowires and In_2O_3 powder). The first shell is In-O shell, the second and the third shell is In-In shell[24]. The In-In shell in the nanowires resembles that of bulk In_2O_3, whereas the In-O shell is markedly smaller than that of bulk In_2O_3, indicting that the interatomic distance between the In and O atoms in In_2O_3 nanowires is reduced. This further confirms that the stronger bond between In and O is formed in the nanowries than that in the powder, which is well consistent with XANES result.

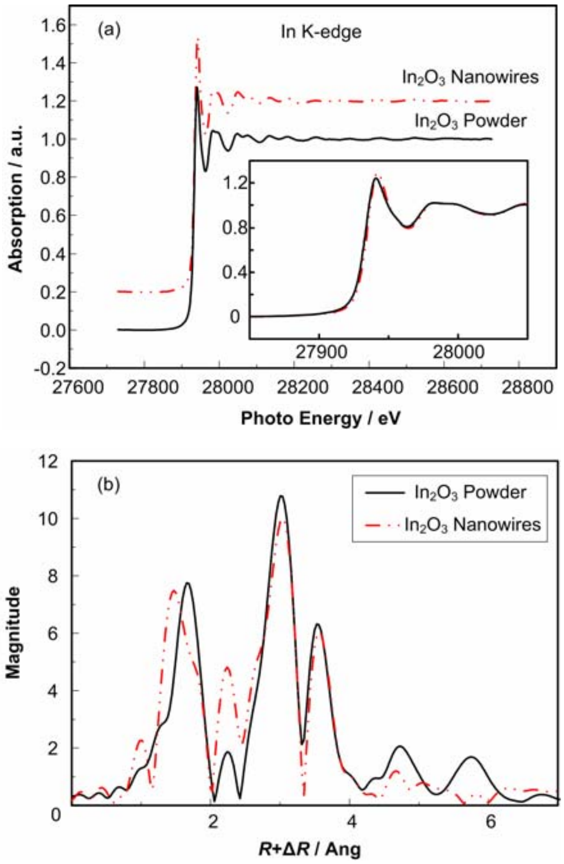

Fig.3 (a) In K-edge XAFS of In_2O_3 nanowire and powder and the XANES is shown the inset. (b) Fourier transform of the XAFS for In_2O_3 nanowire and powder.

Figure 4 shows the oxygen K-edge XANES of In_2O_3 nanowires and In_2O_3 powder. Their features differ distinctly, which indicates that the electronic structure of oxygen in the nanowires is quite different from that of the bulk In_2O_3. There are two O K-edge features, the peak A corresponding to a mixture of O 2*p* and In 5*s* states, and the peak B above 536 eV being due to mixtures of O 2*p* and In 5*p* states[25]. The reduction in peak A and the increase in peak B in the nanowires suggest decreased electron density in the outermost hybrid orbits of O 2*p* and In 5*p* orbits, and movement of *p* electrons to inner hybrid orbits with *s* character. This is consistent with the decreased *p* electrons in In 5*p* orbit in the In K-edge XAFS, due to the stronger In-O bonding in the nanowires.

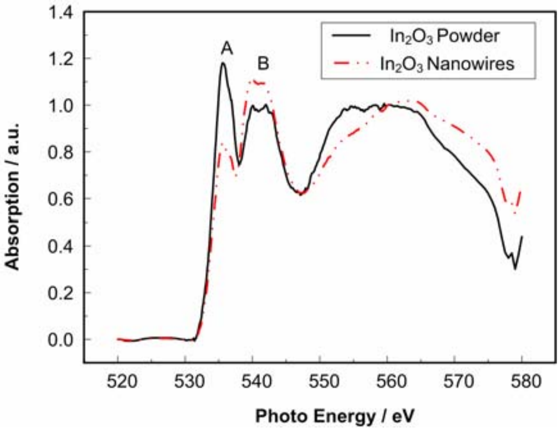

Fig.4 The K-edge spectra of In_2O_3 nanowires and In_2O_3 powder.

Electrical property of the In_2O_3 nanowires was investigated using individual as-synthesized In_2O_3 nanowires to fabricate two terminal devices on 400 nm SiO_2-covered Si substrate with gold pads as the electrodes. Current-voltage (*I-V*) characteristics of the nanowire device were measured by a Keithly 4200CS semiconductor analyzer. Fig.5 shows typical *I-V* curves of an as-synthesized In_2O_3 nanowire. All assynthesized nanowires show similar resistivity in the same order of magnitude. Averaged resistivity of the as-synthesized is 8.79×10^{-4} Ω·m.

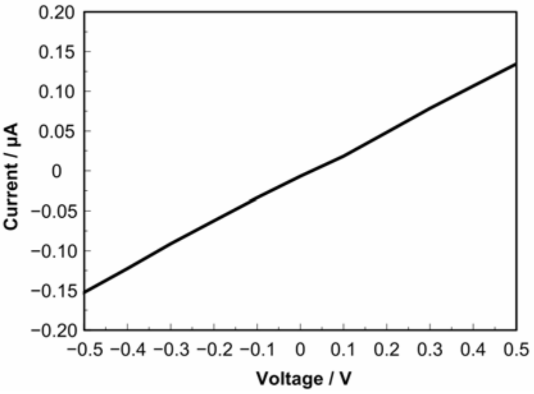

Fig.5 The *I-V* characteristics of one devices fabricated with nanowires of as-synthesized.

Optical luminescence of the In_2O_3 nanowires was studied by photoluminescence (PL) spectroscopy. In Fig.6, a broad PL peak with three shoulders at 380, 465 and 530 nm under the excitation at 280 nm at room temperature was observed. Generally, the PL from oxide semiconductors is mainly attributed to oxygen vacancies[14]. The oxygen vacancies would induce the formation of new energy levels in the band gap. It may be due to the different electronic structure in the In_2O_3 nanowires, too.

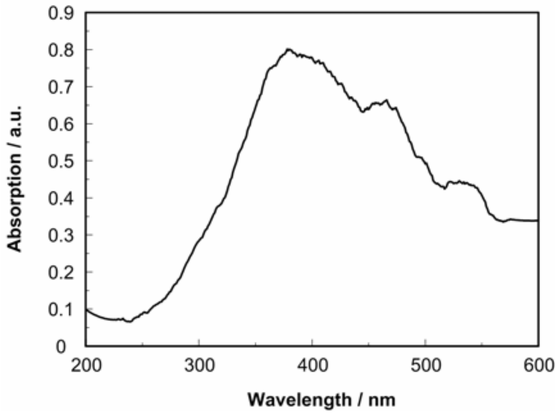

Fig.6 PL spectra of the In_2O_3NWs at room temperature under excitation at 280 nm.

4 Conclusion

Low temperature synthesis of In_2O_3 nanowires with uniform morphology and single crystalline structure is achieved by using InSb as precursor *via* VLS mechanism. The low melting point of InSb and low eutectic point of Au-InSb alloy make it possible to grow In_2O_3 nanowires at temperatures below 450°C. Electronic and local structures of the In_2O_3 nanowires were studied with XAFS. The 5p electrons of In in the In_2O_3 nanowires have tendency to approach to the orbits of O, forming stronger In-O bonding in the nanowires than that in the bulk In_2O_3.

Acknowledgements

The authors thank Dr. Yongfeng Yu at CLS for his insightful discussions. We thank SSRF for providing the beam time of beamlines BL14W (XAFS beamline) and BL14B1 (XRD beamline). Research described in this paper was performed in part at the SGM beamline at Canadian Light Source, which is supported by the NSERC, NRC, CIHR, the Province of Saskatchewan, Western Economic Diversification Canada, and the University of Saskatchewan.

References

1 Huang M H, Wu Y Y, Feick H, *et al.* Adv Mater, 2001, **13:** 113−116.
2 Yuan M R, Chu S Y, Chang R C. Sens Actuator B, 2007, **122:** 269−273.
3 Zeng F H, Zhang X, Wang J, *et al.* Nanotechnology, 2004, **15:** 596−600.
4 Li C, Zhang D H, Liu X L, *et al.* Appl Phys Lett, 2003, **82:** 1613−1615.
5 Li C, Zhang D H, Han S, *et al.* Adv Mater, 2003, **15:** 143−146.
6 Vomiero A, Bianchi S, Comini E, *et al.* Thin Solid Films 2007, **515:** 8356−8359.
7 Li C, Zhang D H, Lei B, *et al.* J Phys Chem B, 2003, **107:** 12451−12455.
8 Zhang D H, Liu Z Q, Li C, *et al.* Nano lett, 2004, **4:** 1919−1924.
9 Chu X F, Wang C H, Jiang D L, *et al.* Chem Phys Lett, 2004, **399:** 461−464.
10 Qurashia A, El-Maghraby E M, Yamazaki T, *et al.* J Alloys Compd, 2009, **481:** L35−L39.
11 Epifani M, Comini E, Arbiol J, *et al.* Sens Actuator B, 2008, **130:** 483−487.
12 Jo G, Hong W K, Maeng J, *et al.* Colloids Surf A, 2008, **313:** 308−311.
13 Wu X C, Hong J M, Han Z J, *et al.* Chem Phys Lett, 2003, **373:** 28−32.
14 Zhang Y F, Li J Y, Li Q, *et al.* Scripta Mater, 2007, **56:** 409−412.
15 Vomiero A, Bianchi S, Comini E, *et al.* Cryst Growth Des, 2007, **7:** 2500−2504.
16 Liang C H, Meng G W, Lei Y, *et al.* Adv Mater, 2001, **13:** 1330−1333.
17 Liu Y K, Yang W G, Hou D D. Superlattices Microstruct, 2008, **43:** 93−100.
18 Zhang J, Qing X, Jiang F H, *et al.* Chem Phys Lett, 2003, **371:** 311−316.
19 Jeong J S, Lee J Y, Lee C J, *et al.* Chem Phys Lett, 2004, **384:** 246−250.
20 Sham T K. Int J Nanotechnol, 2008, **5:** 1194−1246.
21 Sun X H, Wang N B, Li C P, *et al.* Chem Mater, 2004, **16:** 1143−1152.
22 Liu W E, Mohney S E. Mater Sci Eng B, 2003, **103:** 189−201.
23 Prince A, Raynor G V, Evans D S. Phase Diagrams of Ternary Gold Alloys. London (UK): Institute of Metal, 1990, 480−483.
24 Hoel C A, Gaillard J -F, Poeppelmeier K R. J Solid State Chem, 2010, **183:** 761−768.
25 McGuinness C, Stagarescu C B, Ryan P J, J.E. *et al.* Phys Rev B, 2003, **68:** 165104-1-165104-10.